CWI Quarterly Volume 9 (1 & 2) 1996, pp. 77 – 84

Mathematical Modelling in Applied Analysis

E. van Groesen

Faculty of Applied Mathematics, University of Twente
POBox 217, 7500 AE Enschede, The Netherlands
e-mail: groesen@math.utwente.nl

Mathematical modelling in applied analysis refers to exploiting mathematical knowledge about (classes of basic) equations with the aim to describe and analyse phenomena that appear in the natural and technical sciences. As an example we will show that low dimensional models can be derived for phenomena that appear in (perturbations of) dynamical Poisson systems with symmetries. We show that the specific Poisson structure makes it possible to define a manifold of relative equilibria. This manifold, consisting of solutions of the unperturbed equation, is used as a model manifold into which evolutions of perturbed equations can be projected. It turns out that for small perturbations that can have a large effect on the time- and space scales we are interested in, Fredholm solvability conditions determine the projection and hence the final model. We illustrate the ideas to two spatially inhomogeneous systems from fluid dynamics: distorting waves over uneven bottom and swirling flows in expanding pipes. More details about these and other problems can be found in [3, 6].

1. General outline: perturbation theory on model manifold

Consider quite generally an infinite dimensional evolution equation (a partial differential equation in the applications) written like

$$\mathcal{E}_0(u) \equiv \partial_t u - K(u) = 0$$

where u is the state variable, and K the vector field. We assume that for this unperturbed system a smooth manifold of exact solutions is known; with p the parameters characterising the solutions, we get a parameterised manifold of solutions that will be used as the model-manifold in the following:

$$\mathcal{M} = \{U(p) \mid p \in \mathbb{R}^s\}.$$

An immediate consequence is that the evolution operator is degenerate on $\mathcal{M}$:

$$\mathcal{E}_0(U(p)) = 0 \Rightarrow \mathcal{E}_0'(U(p))\frac{\partial U}{\partial p} = 0.$$

Stated differently, the tangent space to $\mathcal{M}$ consists of solutions $\partial U/\partial p$ of the linearized equation $\mathcal{E}_0'(u)\xi \equiv \partial_t\xi - K'(u)\xi = 0$, where K' is the linearised vector field.
Now consider a perturbation of the system, described by

$$\mathcal{E}_\varepsilon(u) \equiv \partial_t u - K_\varepsilon(u) = 0,$$

where K_ε is a small perturbation, measured by the quantity ε, roughly $K_\varepsilon - K = \mathcal{O}(\varepsilon)$.
The aim is to see the relevance of the original invariant manifold $\mathcal{M}$ for the perturbed equation. More specifically, we will look for approximate solutions of the perturbed system as *quasi-homogeneous, or quasi-static evolutions in* $\mathcal{M}$: trajectories in $\mathcal{M}$

$$t \mapsto \bar{u}(t) = U(p(t)),$$

determined by the parameter evolution $t \mapsto p(t)$, for which the error $\eta \equiv u - \bar{u}$ is small, $\eta = \mathcal{O}(\varepsilon)$. On time and space intervals on which the effect of the perturbation on the total solution is large (of order one) this means that we look for approximations that are *uniformly* valid.
A straight forward *error analysis* $0 = \mathcal{E}_\varepsilon(\bar{u}+\eta) = \mathcal{E}_\varepsilon(\bar{u}) + \mathcal{E}_0'(\bar{u})\eta + h.o.t.$ leads to the investigation of the linearized equation:

$$\mathcal{E}_0'(\bar{u})\eta = -\mathcal{E}_\varepsilon(\bar{u}).$$

Here $\mathcal{E}_\varepsilon(\bar{u})$ is recognized as the *residue* of the approximation. Since ε is small, this residue will be of the same order: $\mathcal{E}_\varepsilon(\bar{u}) = \mathcal{O}(\varepsilon)$.
Observe that if the unperturbed linearised operator would be boundedly invertible, it would follow immediately that η is of the required order. But the degeneracy of $\mathcal{E}_0'(\bar{u})$ leads to specific conditions. Indeed, from $\mathcal{E}_\varepsilon(\bar{u}) \in \text{range}[\mathcal{E}_0'(\bar{u})]$ it follows that necessarily the following orthogonality conditions have to be satisfied:

$$\mathcal{E}_\varepsilon(\bar{u}) \perp \ker[\mathcal{E}_0'(\bar{u})^*]$$

where the kernel of the adjoint linearized equation appears: $\mathcal{E}_0'(\bar{u})^*\zeta \equiv -\partial_t\zeta - K'^*(\bar{u})\zeta = 0$. These conditions are necessary, and also sufficient if the linearized operator is a Fredholm operator. In the applications, the operator is indeed of Fredholm type of order zero, and the number of orthogonality conditions (the dimension of the kernel of the adjoint) equals the dimension of the kernel of the linearised operator. We will refer to the conditions as *Fredholm solvability conditions.*
The Fredholm solvability conditions provide $s = \dim(\ker[\mathcal{E}_0'(\bar{u})^*])$ conditions for the evolution of the s parameters p; hence these conditions determine in principle the *parameter dynamics* $t \mapsto p(t) \in \mathbb{R}^s$, and therefore the approximate evolution in $\mathcal{M}$.

1.1. Applicability

To be applicable in problems from mathematical physics, the general outline sketched above rests on two basic assumptions: the possibility to find a model manifold of exact solutions of the unperturbed system, and the possibility to characterize the solutions of the adjoint linearised equation in order to transform the solvability conditions into explicit equations for the parameter dynamics. It seems that at this stage of development, there are two classes of equations for which both assumptions can be satisfied.

One class are gradient-type of systems for which the manifold consists of equilibrium solutions that depend on several parameters, and for which the kernel of the adjoint linearised equation coincides with that of the linearised equation, the latter being known from the degeneracy. Typical examples are pattern formation equations, which have phase-diffusion equations as the determining parameter dynamics; also systems for which the Nonlinear Schrödinger equation for the amplitude appears as solvability condition can be phrased in the general outline above.

A second class of systems are those with a Poisson structure and additional symmetries. In the past years we have shown that various examples can be studied in this way; the model manifold $\mathcal{M}$ is naturally found as the *manifold of relative equilibria*, and the adjoint kernel can be characterised explicitly. In the next section we briefly describe these aspects.

2. Poisson systems with symmetry

The evolution equation of a system with Poisson structure reads

$$\mathcal{E}_0(u) \equiv \partial_t u - \Gamma \delta H(u) = 0$$

where H is a functional, the Hamiltonian (which is in many applications the energy of the system), $\delta H(u)$ denotes its variational derivative, and $\Gamma = \Gamma(u)$ is a "structure map", i.e. a skew symmetric operator such that $\{ F, G \}(u) := \langle \delta F(u), \Gamma \delta G(u) \rangle$ is a Poisson bracket (satisfies Jacobi's condition). (If Γ is non-degenerate, the system is Hamiltonian; in several interesting problems the map is degenerate). We will denote the Hamiltonian flow by $u(t) = \Phi_t^H(u_0)$ for the solution with initial condition u_0. For such systems, the Hamiltonian (energy) is a constant of the motion (first integral): $H(\Phi_t^H(u_0)) = H(u_0)$, for all t. Special solutions, *equilibria*, time-independent solutions, are found as critical points of the Hamiltonian: $\hat{u} \in \text{Crit } \{ H(u) \mid u \in \mathcal{U} \}$, for which $\delta H(\hat{u}) = 0$; in many applications the energy-minimizers are relevant, but are non-degenerate and cannot be used as a model manifold. However, when an additional symmetry, or degeneracy is present, there are other solutions that will form a model manifold.

Suppose that, except H, there is an additional first integral I. A particular case may be a *Casimir functional* C which satisfies $\{C, F\} = 0$ for all F, i.e. for which $\Gamma \delta C \equiv 0$; these Casimir functionals can appear only in degenerate Poisson systems. The flow of an integral I, Φ^I, is a continuous *symmetry*; it is

trivial for Casimirs functionals. (For simplicity of exposition we describe in this section the case of one additional integral; the extension to more integrals is rather straightforward, in particular when the symmetry flows mutually commute.)
In a natural way, for Poisson systems with symmetry one can define a *manifold of relative equilibria* MRE along the following lines. Relative equilibria RE are found from a *Constrained Energy Principle*: prescribing the value of the additional integral, critical points (minimizers to guarantee some stability properties) of the energy on the level set

$$U(\gamma) \in \text{Min } \{\ H(u) \mid\ I(u) = \gamma\ \}, \quad \delta H(U) = \lambda \delta I(U)$$

are for each γ degenerate by the I-flow (when nontrivial). Taking the action of the flow (parameterised by φ) and the value of the constraint as parameters, one obtains the MRE as the set

$$\mathcal{M} = \{U(\gamma, \varphi) \equiv \Phi^I_\varphi U(\gamma) \mid \gamma, \varphi\}.$$

This MRE consists of dynamic evolutions, the so-called *relative equilibrium solutions*, which are simply evolutions along the group orbit: $\Phi^I_{\lambda t}(U(\gamma, \varphi_0)) = U(\gamma, \varphi_0 + \lambda(\gamma)t)$; the speed λ is precisely the Lagrange multiplier that appears in the equation for the constrained critical point.
Taking this set $\mathcal{M}$ as the model manifold, the general theory predicts the degeneracy, which consists of an expected degeneracy along the symmetry flow $\Gamma \delta I(U)$, but also of a degeneracy perpendicular to the level set of I, given by $\partial U / \partial \gamma$.
The elements from the kernel of the adjoint linearised equation are more difficult to find. It is known, see e.g. Lax, [8], that the variational derivative of an integral, $\delta I(u)$, evolves with the adjoint flow. In general, the following results holds for any Poisson system.

KERNEL THEOREM ([4])
For the Poisson system it holds that

$$\begin{aligned} [\mathcal{E}_0'(u)\Gamma(u)]^* &= \mathcal{E}_0'(u)\Gamma(u); \ \textit{consequently:} \\ \ker[\mathcal{E}_0'(u)^*] &= -\Gamma(u)^{-1}_{pseudo} \ker[\mathcal{E}_0'(u)], \end{aligned}$$

where the inverse $\Gamma(u)^{-1}_{pseudo}$ has to be interpreted as a pseudo-inverse in case there are Casimir functionals.

This brief description shows that for Poisson systems with symmetry both assumptions for the applicability of the general ideas can be met in a natural way.

3. APPLICATIONS

We have applied the above ideas to Poisson systems with various kinds of perturbations. Systems with small *dissipation* concerned surface waves and plane

flows: the decay of soliton-like solutions in the perturbed Korteweg - de Vries equation, the self-organization in plane flows and the viscous decay of vortices in the Navier - Stokes equation.
In this contribution we describe two systems with *spatial inhomogeneity*; another example, the particle model for Bloch boundaries in inhomogeneous ferromagnetic material, is described in [3].
For these inhomogeneous systems the perturbed equation is a Poisson system itself; the inhomogeneity is characterized by a function, say $\kappa = \kappa(x)$, which is the depth $h(x)$ in the wave problem, and the radius of the pipe $R(z)$ in the swirling flow problem. The model manifold now consists of the union of manifolds of relative equilibria of the homogeneous problems for which κ is a constant; this introduces an additional parameter. We will not go into details but restrict ourselves to describe some of the results in the next subsections.

3.1. Waves above topography

In a good approximation, gravity driven surface waves on a layer of fluid above a horizontal bottom are described by the Korteweg - de Vries equation. This equation has a Hamiltonan structure, with the energy as Hamiltonian. Their are many symmetries, actually infinitely many since KdV is completely integrable. The one of interest here is translation for which the horizontal momentum is the corresponding constant of the motion. The relative equilibria are in this case the solitary wave (shapes), the solitons, that can be characterized variationally like

$$U(h;\gamma,\varphi) \in \text{Min } \{ \text{ Energy } | \text{ Hor. momentum} = \gamma \} .$$

Here h is the depth and φ denotes the "position" of the wave; the amplitude of the wave is related in a one to one way with the value γ. A translation with speed λ (depending on γ) is the actual travelling wave.
For each depth h, the solitary waves determine a two-dimensional manifold; more dimensional MRE's can be obtained by prescribing more integrals, for instance the manifold of two-solitons.
The description of waves above a varying bottom is more involved; when the topography changes on a scale larger then the effective wavelength of the waves, a modification of the KdV-equation is valid (see [7, 9]). This modification is still a Hamiltonian system; the coefficients depend on the depth function $h(x)$. Since translation symmetry is lost, the horizontal momentum is not a first integral anymore, and a solitary wave will deform. With Pudjaprasetya we studied this deformation in detail. In particular for a wave running into shallower water, the results are interesting. In the literature the common approach is to take some simple model for the change of the wave form during the running up, and then study the fission of the deformed, single, wave on the new (smaller) depth using inverse scattering theory for KdV. Depending on the change in depth, two or more solitary waves emerge, as is well known for KdV on a horizontal bottom. We have described the process of running up in a different way by using the

quasi-homogeneous approximation in the manifold of two-solitons (or, almost as accurate, as the simple superposition of two single solitary waves), and deriving the parameter dynamics from the solvability conditions. The results turn out to be in good agreement with numerical calculations that were performed to verify this analytical approximation ([1]). In Figure 1 the results of these numerical calculations by Van Daalen are shown; for the change in depth considered, the splitting of the solitary wave in two solitary waves (and a small tail) is clearly visible. (Actually, for the numerical calculations, the complete set of surface wave equations is used instead of the KdV-approximation; the results agree remarkably well.)

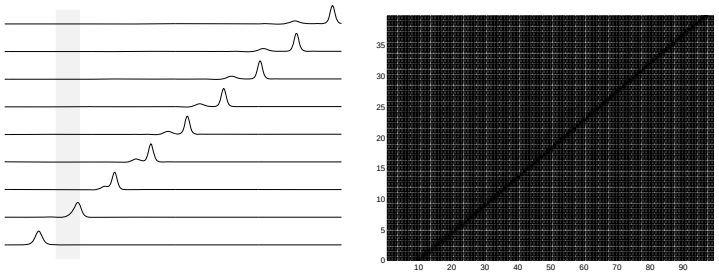

FIGURE 1. At the left, several wave profiles (shifted vertically for increasing time) show the splitting process; the grey band indicates the area of decrease in depth. At the right the elevation of the waves is indicated by grey scales.

3.2. Swirling flow in expanding pipes

To support the design of industrial burners (for instance to reduce the production of noxious pollutants), a detailed knowledge of the flow is required. The main interest, and least understood aspect, concerns the appearance of *recirculation areas* in swirling flows. This problem is related to the problem of vortex breakdown in swirling flows without boundaries.

Assuming the flow to be inviscid and incompressible, the governing equations are the three dimensional Euler equations of fluid dynamics. Restricting to flows in circularly symmetric pipes, rotation symmetry can be invoked. The Euler equations are a Poisson system, with the kinetic energy as Hamiltonian. An important Casimir functional is the *helicity*, a quantity that measures the knottedness of streamlines. The axial flux is another first integral, with axial translation as its flow. In a cylindrical pipe with constant radius, several discrete manifolds of relative equilibria can be found. These relative equilibria, called critical swirling flows, are the variants of the solitons in the wave problem above; they are the constrained critical points of the energy:

$$\text{Crit } \{ \text{ Energy } | \text{ Helicity} = b, \quad \text{Axial flux} = f \ \}.$$

(Here the functionals are integrals over a cross section of the pipe.) Among the relative equilibria, which can be given explicitly in terms of Bessel functions, two main families of solutions can be distinguished; the axial and angular velocity profiles (uniform in the angular and axial direction) of these primary flows are shown in Figure 2.

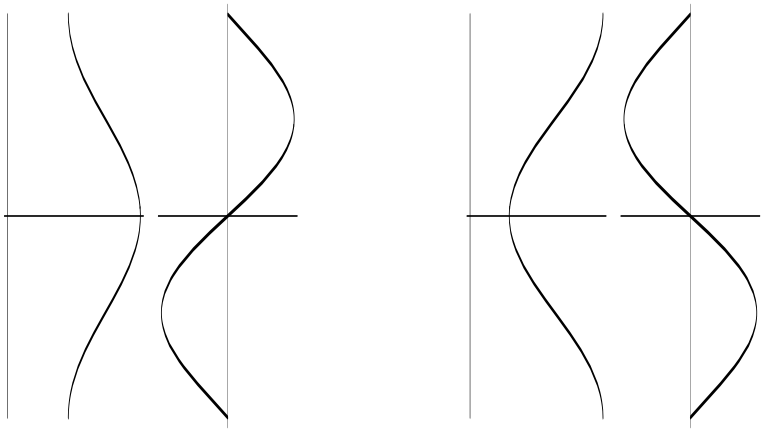

FIGURE 2. For given helicity and axial flux, shown are the axial and angular velocity profiles of the co-rotating primary flow (at the left) and of the counter-rotating primary flow (at the right).

In an expanding pipe, the axial translation symmetry is lost and the flows will deform. Using a quasi-homogeneous approximation we studied, with Van de Fliert and Fledderus, the development of the flow; from the solvability conditions the change in the values of the constraints as a function of the changing radius was determined ([5]; see also [2]). Stated differently, the flows are found as solutions of the Bragg-Hawthorn equation, where the functions that appear in this equation, the head and circulation, change in a specified way with changing pipe radius.
The results show that a characteristic difference can be observed for the two primary flows: the co-rotating flow (for which $b\omega^z$, helicity times axial vorticity component, is positive) develops a recirculation area near the wall of the pipe, while the counter-rotating flow (for which $b\omega^z < 0$) develops a recirculation near the axis. The latter result agrees quite well with experimental findings (performed at Mechanical Engineering, UT, [10]); the recirculation areas near the wall may correspond to flows that loose their stability (separation of the boundary layer); further research by Fledderus, in progress, concerns stability investigations for the various critical flows, the matching of the Eulerian flows to a viscid boundary layer and a detailed comparison with experimental data.

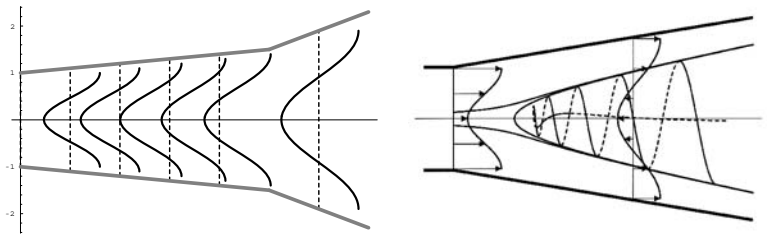

FIGURE 3. Appearance of a recirculation area near the axis in an expanding pipe as calculated in the quasi-homogeneous approximation in the family of the counter-rotating primary flows. An artistic impression of the recirculation area, with the trajectory of a single particle, is shown at the right.

REFERENCES

1. E.F.G. DAALEN, E. VAN GROESEN, S.R. PUDJAPRASETYA (1996). BEM-numerics and KdV-model analysis for solitary wave split-up . *Comp. Math.*.
2. E.R. FLEDDERUS AND E. VAN GROESEN (1995). Quasi-homogeneous critical swirling flows in expanding pipes, Part II. *J. Math. Anal. Appl., accepted.*
3. E.R. FLEDDERUS AND E. VAN GROESEN (1996). Deformation of coherent structures. *Rep. Progr. Phys.* **59**: 1–89.
4. E. VAN GROESEN (1995). A Hamiltonian perturbation theory for coherent structures illustrated to wave problems. In A. MIELKE AND K KIRCHGASSNER, editors, *Structure and dynamics of nonlinear waves in Fluids*, pages 99–116. Springer.
5. E. VAN GROESEN, B.W. VAN DE FLIERT, E.R. FLEDDERUS (1995). Quasi-homogeneous critical swirling flows in expanding pipes. *J.Math.Ann.Appl.* **192**: 764–788.
6. E. VAN GROESEN AND E.M. DE JAGER (1994). *Mathematical structures in continuous dynamical systems.* North–Holland, Elsevier, Amsterdam.
7. E. VAN GROESEN AND S.R. PUDJAPRASETYA (1993). Uni-directional waves over slowly varying bottom. Part I: Derivation of a KdV-type of equation. *Wave Motion* **18**: 345–370.
8. P.D. LAX (1968). Integrals of nonlinear equations of evolution and solitary waves. *C.P.A.M.* **XXI**: 467–490.
9. A.C. NEWELL (1985). *Solitons in mathematics and physics.* SIAM, Philadelphia.
10. F.J.J. ROSENDAL (1993). *Swirling flows in expanding tubes.* University of Twente.